

Chiral anomaly and internode scatterings in multifold semimetals

Ipsita Mandal*

Department of Physics, Shiv Nadar Institution of Eminence (SNIOE),
Gautam Buddha Nagar, Uttar Pradesh 201314, India

In our quest to unravel the topological properties of nodal points in three-dimensional semimetals, one hallmark property which warrants our attention is the *chiral anomaly*. In the Brillouin zone (BZ), the sign of the Berry-curvature field's monopole charge is referred to as the chirality (χ) of the node, leading to the notion of *chiral quasiparticles* sourcing *chiral currents*, induced by internode scatterings proportional to the chiral anomaly. Here, we derive the generic form of the chiral conductivity when we have multifold nodes. Since the sum of all the monopole charges in the BZ are constrained to vanish, the nodes appear in pairs of $\chi = \pm 1$. Hence, the presence of band-crossing degeneracies of order higher than two make it possible to have two distinct scenarios — the pair of conjugate nodes in question comprise bands of the same pseudospin variety or of two distinct pseudospin-representations. Covering these two possibilities, we apply our derived formula to semimetals harbouring triple-point (threefold-degenerate) and Rarita-Schwinger-Weyl (fourfold-degenerate) nodes, and show the resulting expressions for the conductivity featuring the chiral anomaly.

I. INTRODUCTION

There have been continuous efforts, both on the theoretical and experimental fronts, for unravelling the multifaceted exotic properties of three-dimensional (3d) semimetals, which harbour symmetry-protected band-crossing points in the Brillouin zone (BZ) near the Fermi level [1–8]. Since the density-of-states go exactly to zero at the nodal points, the semimetals differ from both the insulators (which always has a gap between the bands) and conventional metals (where bands overlap in finite regions of the BZ, with a finite density of states). In general, the low-energy effective Hamiltonian of a system in the vicinity of a band-crossing point, with $(2\zeta + 1)$ bands converging there, can be expressed as

$$\mathbf{d}(\mathbf{k}) \cdot \mathcal{S}, \quad \mathbf{d}(\mathbf{k}) = \{d_x(\mathbf{k}), d_y(\mathbf{k}), d_z(\mathbf{k})\}, \quad (1)$$

in the 3d momentum space ($\mathbf{k} = \{k_x, k_y, k_z\}$). Here, the vector operator $\mathcal{S} \equiv \{\mathcal{S}_x, \mathcal{S}_y, \mathcal{S}_z\}$ represents the three components of the angular momentum operator in the spin- ζ representation of the SU(2) group. This is precisely the so-called $\mathbf{k} \cdot \mathbf{p}$ Hamiltonian, which can be obtained by performing *ab initio* simulations for determining the bandstructures of the relevant materials. The emergent quasiparticles carry a set of quantum numbers, which we call pseudospin (ζ). The terminology of *pseudospin* has been coined so as to unambiguously distinguish it (arising from crystal symmetries) from the relativistic spin (arising from the spacetime Lorentz invariance). In particular, the cases of multifold-band-crossing points have been identified in the 65 chiral space groups characterizing the chiral crystals [6], which are the ones with only orientation-preserving symmetries. When the dominant terms involve linear-in-momentum dispersion, we have $\mathbf{d}(\mathbf{k}) = \mathbf{k}$. Such examples include the nodes of a (1) pseudospin-1/2 Weyl semimetal (WSM) [1, 2, 9], (2) pseudospin-1 triple-point semimetal (TSM) [4, 6, 8, 10–16], (3) pseudospin-3/2 Rarita-Schwinger-Weyl semimetal (RSM) [4, 6, 8, 10, 13–15, 17–26]. They involve two, three, and four bands crossing at the nodal point, respectively (as embodied in the value of ζ), and will constitute the example-systems that we will consider in this paper. It is interesting to note that, unlike the WSMs, integer- ζ quasiparticles (with odd number of bands crossing at a nodal point) have no analogs in high-energy physics, since the occurrence of integer-spin relativistic fermions is naturally prohibited by the spin-statistics theorem. The wide range of transport signatures, that have been extensively investigated heretofore, include intrinsic anomalous-Hall effect [27–29], nonzero planar-Hall response [3, 8, 25, 26, 30–47], magneto-optical conductivity under quantizing magnetic fields [48–50], Magnus Hall effect [22, 51, 52], circular dichroism [13, 53], circular photogalvanic effect [54–57], and transmission of quasiparticles across potential barriers/wells [23, 58–60]. Such overwhelming literature has been fuelled by the fact that the 3d nodal-point semimetals are generically associated with nontrivial topology in the 3d momentum space, giving rise to vector fields in the forms of Berry curvature (BC) and orbital magnetic moment (OMM). These intrinsic topological quantities stem from the Berry phase [3, 8, 25, 26, 43–47, 61–63] and, when probed by externally-applied fields, lead to unique signatures by the virtue of affecting the response tensors.

For a nodal-point semimetal harbouring nontrivial topology, the nodes act as the singular points of the BC field, such that the converging/emanating bands carry BC monopoles [64, 65], demarcating topological defects carrying nonzero topological charges. The sign of the monopole charge is referred to as the chirality χ of the node, leading to the notion of *chiral* quasiparticles. We call them *right-handed* or *left-handed*, depending on whether $\chi = 1$ or $\chi = -1$. The sum of all the monopole charges, carried by either the conduction or valence bands of all the chirally-charged nodes in the BZ, are constrained to

* ipsita.mandal@snu.edu.in

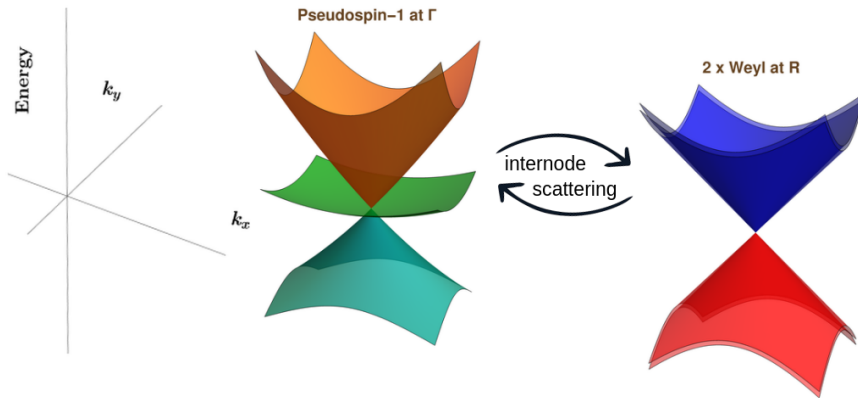


FIG. 1. Schematics of the multiple bands of a single pseudospin-1 triple-point node (at the Γ -point) and a double-pseudospin-1/2 node (at the R -point) against the $k_x k_y$ -plane. The internode scatterings, thus, involve bands having distinct topological properties, although the monopole charge (summed over either the conduction or the valence bands) from one node is the negative of the other.

vanish. This is in agreement with the Nielsen-Ninomiya theorem [66]. Here, we adopt the convention that χ refers to the sign of the monopole charges of the negative-energy bands (i.e., the valence bands).¹ Our convention implies that a positive (negative) sign indicates that the node acts as a source (sink) for the field lines of the BC.

In the context of high-energy physics, the relativistic Weyl fermions possesses the hallmark property of the chiral anomaly, also known as the Adler-Bell-Jackiw anomaly of quantum electrodynamics [67, 68]. Strikingly, the phenomenon continues to hold in nonrelativistic settings involving WSMs [69–71] and its higher-pseudospin generalizations (i.e., multifold nodal points) [8]. In fact, for the low-energy physics governing condensed-matter systems, the anomaly reduces to the process of chiral-charge pumping from one node (which chirality χ) to its conjugate (with chirality $-\chi$), when we subject the material to external electric (\mathbf{E}) and magnetic (\mathbf{B}) fields. Since the rate of pumping is proportional to $\mathbf{E} \cdot \mathbf{B}$, we need $\mathbf{E} \cdot \mathbf{B} \neq 0$ to cause a net imbalance of chiral quasiparticles in the vicinity of an individual node. Of course, the total number of quasiparticles, obtained by summing over the conjugate pairs of nodes in the entire BZ, must yield zero, as required to conserve the net electric charge. In other words, a net chiral current must appear as a purely quantum-mechanical effect (due to $\mathbf{E} \cdot \mathbf{B} \neq 0$), although the total particle current must vanish.

In this paper, we apply the semiclassical Boltzmann formalism [3, 25, 43], using the relaxation-time approximation, to determine the chiral current induced by the chiral anomaly, in the regime of nonquantizing magnetic fields. This involves considering a collision integral (I_{coll}) which contains a part ($I_{\text{coll}}^{\text{inter}}$) induced by internode scatterings. While earlier works [34, 72] have considered this problem (specifically, for WSMs), the issue of scattering between nodes of multifold nodal points have not been addressed. For multifold degeneracies, we encounter two distinct situations: (1) the pair of conjugate nodes in question are of the same pseudospin variety; (2) the pair of conjugate nodes comprise bands of different pseudospin quantum numbers. The first case is exemplified by a pair of TSMS [4, 11]. The second case is exemplified by the following two realizations:

- (a) A single node of TSM is pinned at the center of the BZ (i.e., the Γ -point), carrying a monopole charge of $+2$, while a fourfold-degenerate node (comprising two copies of WSMs of the same chirality) exists at the boundary of the BZ (i.e., the R -point) with a net monopole charge equalling $-1 - 1 = -2$. This is shown schematically in Fig. 1. Candidate materials include CoSi [8].
- (b) An RSW node is pinned at the Γ -point, carrying a monopole charge of $+4$, while a sixfold-degenerate node (comprising two copies of TSMs of the same chirality) exists at the R -point with a net monopole charge equalling $-2 - 2 = -4$. This is shown schematically in Fig. 2. Candidate materials include the SrGePt family (e.g., SrSiPd, BaSiPd, CaSiPt, SrSiPt, BaSiPt, and BaGePt) [15].

The paper is organized as follows: In Sec. II, we describe the derivation of the generic expression of the conductivity tensor ($\sigma_s^{\chi, \text{inter}}$), which is connected to the chiral-charge pumping induced by the chiral anomaly. Sec. III is devoted to finding the explicit expressions for $\sigma_s^{\chi, \text{inter}}$, considering some specific systems (described above). Finally, we end with a summary and some future perspectives in Sec. IV. We provide the details of various expressions/intermediate steps in the appendices. Throughout the paper, we will be using natural units.

¹ The nomenclature of “conduction” (positive-energy) and “valence” (negative-energy) bands refers to the signs of the dispersion measure with respect to the nodal point (where we set the zero of energy).

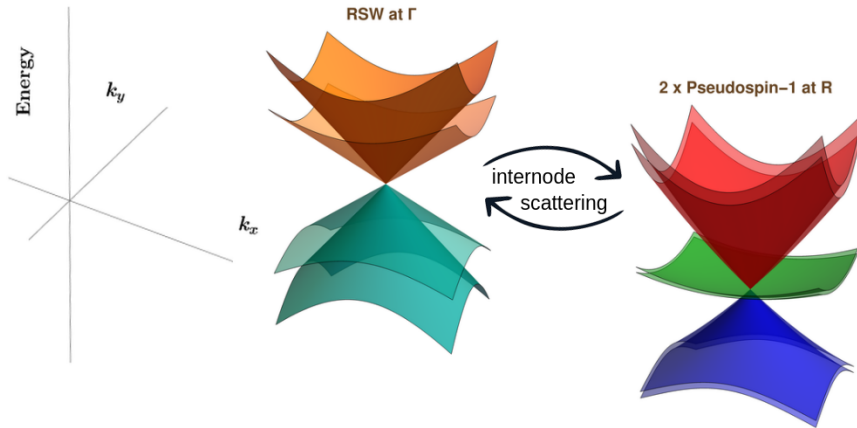


FIG. 2. Schematics of the multiple bands of a single RSW node (at the Γ -point) and a double-pseudospin-1 triple-point node (at the R -point) against the $k_x k_y$ -plane. The internode scatterings, thus, involve bands having distinct topological properties, although the monopole charge (summed over either the conduction or the valence bands) from one node is the negative of the other.

II. BOLTZMANN FORMALISM

Let us consider the transport by quasiparticles in the vicinity of the node with chirality χ in a 3d nodal-point semimetal. Let us define the distribution function by $f_s^\chi(\mathbf{r}, \mathbf{k}, t)$ for the quasiparticles occupying a Bloch band labelled by the index s , with the crystal momentum \mathbf{k} , band-dispersion $\varepsilon_s^\chi(\mathbf{k})$, and group velocity $\mathbf{v}_s^\chi(\mathbf{k}) = \nabla_{\mathbf{k}} \varepsilon_s^\chi(\mathbf{k})$. In general, where we do not have nodes of the same nature for χ and $-\chi$, s is a function of χ [i.e., $s = s(\chi)$]. However, for uncluttering the notations, we suppress the χ -dependence of the s -index, and it will be clear from the χ -index of the relevant quantities what values of s we are talking about. If $\Omega_s^\chi(\mathbf{k})$ is the associated BC, then

$$\mathcal{D}_s^\chi(\mathbf{k}) = \frac{1}{1 + e[\mathbf{B} \cdot \Omega_s^\chi(\mathbf{k})]} \quad (2)$$

is the factor which modifies the phase volume element from $dV_p(\mathbf{r}, \mathbf{k}) \equiv \frac{d^3 \mathbf{k}}{(2\pi)^3} d^3 \mathbf{r}$ to $[\mathcal{D}_s^\chi(\mathbf{k})]^{-1} dV_p(\mathbf{r}, \mathbf{k})$, such that the Liouville's theorem (in the absence of collisions) continues to hold in the presence of a nonzero BC [71, 73–75]. Hence, the modified classical probability density of the phase space, centered at $\{\mathbf{r}, \mathbf{k}\}$ at time t , is given by

$$dN_s^\chi(\mathbf{r}, \mathbf{k}) = g_s [\mathcal{D}_s^\chi(\mathbf{k})]^{-1} f_s^\chi(\mathbf{r}, \mathbf{k}, t) dV_p(\mathbf{r}, \mathbf{k}). \quad (3)$$

Here, g_s denotes the degeneracy of the band.

Let us define

$$\xi_s^\chi(\mathbf{k}) = \varepsilon_s^\chi(\mathbf{k}) + \eta_s^\chi(\mathbf{k}), \quad \eta_s^\chi(\mathbf{k}) = -\mathbf{m}_s^\chi(\mathbf{k}) \cdot \mathbf{B}, \quad \mathbf{w}_s^\chi = \mathbf{v}_s^\chi + \mathbf{u}_s^\chi(\mathbf{k}), \quad \mathbf{u}_s^\chi(\mathbf{k}) = \nabla_{\mathbf{k}} \eta_s^\chi(\mathbf{k}), \quad (4)$$

where $\mathbf{m}_s^\chi(\mathbf{k})$ is the OMM and $\eta_s^\chi(\mathbf{k})$ is the OMM-induced correction to the effective dispersion. Similarly, $\mathbf{w}_s^\chi(\mathbf{k})$ is the OMM-corrected the band velocity. Using the explicit forms of the solutions for f_s^χ [32, 34], the contribution to the electric current density from the s^{th} is captured by

$$\begin{aligned} \mathbf{J}_s^\chi &= -e g_s \int \frac{d^3 \mathbf{k}}{(2\pi)^3} (\mathcal{D}_s^\chi)^{-1} \dot{\mathbf{r}} f_s^\chi(\mathbf{r}, \mathbf{k}) \text{ and } \mathbf{J}_s^{\text{th}, \chi} = g_s \int \frac{d^3 \mathbf{k}}{(2\pi)^3} (\mathcal{D}_s^\chi)^{-1} \dot{\mathbf{r}} (\xi_s^\chi - \mu_\chi) f_s^\chi(\mathbf{r}, \mathbf{k}) \\ \Rightarrow \mathbf{J}_s^\chi &= -e g_s \int \frac{d^3 \mathbf{k}}{(2\pi)^3} [\mathbf{w}_s^\chi + e(\mathbf{E} \times \Omega_s^\chi) + e(\Omega_s^\chi \cdot \mathbf{w}_s^\chi) \mathbf{B}] f_s^\chi(\mathbf{r}, \mathbf{k}). \end{aligned} \quad (5)$$

Henceforth, we will set $g_s = 1$, assuming nondegenerate bands (away from the nodal points where the bands cross) and ignoring any electronic spin-degeneracy.

A. Solution in the absence of internode scattering

The Fermi-Dirac distribution function

$$f_{s,\chi}^{(0)}(\mathbf{r}, \mathbf{k}) \equiv f_{(0)}(\xi_s^\chi(\mathbf{k}), \mu_\chi, T) = \frac{1}{1 + \exp\left[\frac{\xi_s^\chi(\mathbf{k}) - \mu_\chi}{T}\right]}, \quad (6)$$

describes a local equilibrium situation at the subsystem centred at position \mathbf{r} , at the local temperature $T(\mathbf{r})$, and with a spatially uniform chemical potential μ_χ . We consider the situation where T and μ_χ are constants. In order to obtain a solution to the full Boltzmann equation for small $|\mathbf{E}|$, we assume a small deviation, $\delta f_s^X(\mathbf{k})$, from the equilibrium distribution. We have not included any explicit time or spatial dependence in it since \mathbf{E} is static. Hence, the nonequilibrium time-independent distribution function can be expressed as

$$f_s^X(\mathbf{r}, \mathbf{k}, t) \equiv f_s^X(\mathbf{k}) = f_{(0)}(\xi_s^X(\mathbf{k})) + \delta f_s^X(\mathbf{k}), \quad (7)$$

where we have suppressed showing explicitly the dependence of $f_{(0)}$ on μ_χ , and T . At this point, the magnetic field is not assumed to be small, except for the fact that it should not be so large that the energy levels of the systems get modified by the formation of discrete Landau levels.

To unclutter notations, we will use the superscript ‘‘prime’’ to denote differentiation with respect to the variable shown within the brackets [for example, $f'_{(0)}(u) \equiv \partial_u f_{(0)}(u)$]. We work in the linearized approximation (i.e., we keep terms up to the linear order in the ‘‘smallness parameter’’), which implies

$$\nabla_{\mathbf{k}} f_{(0)}(\xi_s^X(\mathbf{k})) = \mathbf{w}_s^X f'_{(0)}(\xi_s^X(\mathbf{k})), \quad (8)$$

assuming that δf_s^X is of the same order of smallness as the external perturbation \mathbf{E} . This leads to the *linearized Boltzmann equation*, given by

$$-e D_s^X [\{\mathbf{w}_s^X + e(\boldsymbol{\Omega}_s^X \cdot \mathbf{w}_s^X) \mathbf{B}\} \cdot \mathbf{E}] f'_{(0)}(\xi_s^X(\mathbf{k})) + e D_s^X \mathbf{B} \cdot (\mathbf{w}_s^X \times \nabla_{\mathbf{k}}) \delta f_s^X(\mathbf{k}) = I_{\text{coll}}, \quad I_{\text{coll}} = -\frac{\delta f_s^X(\mathbf{k})}{\tau}. \quad (9)$$

Here, I_{coll} represents the collision integral, which parametrize by using the phenomenological relaxation-time τ . We want to solve the above equation for our planar Hall configurations by using an appropriate ansatz for $\delta f_s^X(\mathbf{k})$.

We define the Lorentz-force operator as

$$\check{L} = (\mathbf{w}_s^X \times \mathbf{B}) \cdot \nabla_{\mathbf{k}}, \quad (10)$$

such that Eq. (9) can be rewritten as

$$e D_s^X [\{\mathbf{w}_s^X + e(\boldsymbol{\Omega}_s^X \cdot \mathbf{w}_s^X) \mathbf{B}\} \cdot \mathbf{E}] [-f'_{(0)}(\xi_s^X(\mathbf{k}))] - e D_s^X \check{L} \tilde{g}_s^X(\mathbf{k}) \delta f_s^X(\mathbf{k}) = -\frac{\delta f_s^X(\mathbf{k})}{\tau}. \quad (11)$$

The solutions and the resulting conductivity tensors for various semimetals have been extensively studied in our earlier papers [25, 26, 42, 43, 45–47].

B. Solution in the presence of internode scattering

We now discuss how to include internode scatterings in a relaxation-time approximation, where we treat the internode scattering time τ_G as a phenomenological constant (analogous to τ). To start with, let us assume that initially in the infinite past (denoted by time $t = -\infty$) both the nodes had the same chemical potential E_F , characterized by the distribution function

$$f_0(\varepsilon) = \frac{1}{1 + e^{\frac{\varepsilon - E_F}{T}}}, \quad (12)$$

in the absence of any externally applied fields. Eventually, on applying the electromagnetic fields, there is the onset of the chiral anomaly, causing the two nodes to acquire a local equilibrium value of chemical potential given by μ_χ . Therefore, the local equilibrium distribution function at each node is given by

$$f_{s,L}^X \simeq f_0(\xi_s^X) + [-f'_0(\xi_s^X)] \delta\mu_\chi, \quad \delta\mu_\chi \equiv \mu_\chi - E_F. \quad (13)$$

The intranode-part of the collision integral ($I_{\text{coll}}^{\text{intra}}$) tends to drive the quasiparticle distribution towards this value, leading to

$$I_{\text{coll}}^{\text{intra}} = -\frac{f_s^X(\mathbf{k}) - f_{s,L}^X}{\tau}. \quad (14)$$

On the other hand, the internode-part of the collision integral ($I_{\text{coll}}^{\text{inter}}$) tends to relax the quasiparticle distribution towards the global equilibrium of the chemical potential, μ_G , given by

$$f_{s,G}^X \simeq f_0(\xi_s^X) + [-f'_0(\xi_s^X)] \delta\mu_G, \quad \mu_G = \frac{\mu_\chi + \mu_{-\chi}}{2}, \quad \delta\mu_G \equiv \mu_G - E_F = \frac{\delta\mu_\chi + \delta\mu_{-\chi}}{2}. \quad (15)$$

Hence, we get

$$I_{\text{coll}}^{\text{inter}} = -\frac{f_s^\chi(\mathbf{k}) - f_{s,G}^\chi}{\tau_G}. \quad (16)$$

To derive the coefficients of linear response, we parametrize the nonequilibrium distribution function as [76]

$$f_s^\chi(\mathbf{k}) = f_0(\xi_s^\chi) + [-f_0'(\xi_s^\chi)] \tilde{g}_s^\chi(\mathbf{k}), \quad (17)$$

where \tilde{g}_s^χ quantifies the deviation of the chemical potential caused by the external probe fields (which are assumed to be spatially uniform and time-independent). With this definition, the total collision intergral takes the following form:

$$I_{\text{coll}} = I_{\text{coll}}^{\text{intra}} + I_{\text{coll}}^{\text{inter}}, \quad \frac{I_{\text{coll}}^{\text{intra}}}{f_0'(\xi_s^\chi)} = \frac{\tilde{g}_s^\chi(\mathbf{k}) - \delta\mu_\chi}{\tau}, \quad \frac{I_{\text{coll}}^{\text{inter}}}{f_0'(\xi_s^\chi)} = \frac{\tilde{g}_s^\chi(\mathbf{k}) - \delta\mu_G}{\tau_G}, \quad (18)$$

Accordingly, τ and τ_G represent the phenomenological relaxation-times applicable for the intranode and internode scatterings, respectively. Here, we have assumed the same relaxation time for all the bands involved.

Let us also define the average over all the possible electron states (i.e., the expectation value) of a physical observable $\mathcal{O}_s^\chi(\xi_s^\chi(\mathbf{k}), \mu, T)$ as

$$\bar{\mathcal{O}}_\chi \equiv \langle \mathcal{O}_s^\chi(\xi_s^\chi(\mathbf{k}), E_F, T) \rangle = \frac{\sum_s \int \frac{d^3\mathbf{k}}{(2\pi)^3} (\mathcal{D}_s^\chi)^{-1} [-f_0'(\xi_s^\chi(\mathbf{k}))] \mathcal{O}_s^\chi(\xi_s^\chi(\mathbf{k}), E_F, T)}{\sum_s \int \frac{d^3\mathbf{q}}{(2\pi)^3} (\mathcal{D}_s^\chi)^{-1} [-f_0'(\xi_s^\chi(\mathbf{q}))]}. \quad (19)$$

Since the momentum-integrals run over all the quasiparticle-states at the Fermi level of band s for node χ , the quantity

$$\rho_\chi \equiv \sum_s \int \frac{d^3\mathbf{k}}{(2\pi)^3} (\mathcal{D}_s^\chi)^{-1} [-f_0'(\xi_s^\chi(\mathbf{k}))] \quad (20)$$

represents the density of states at node χ [cf. Eq. (3)]. It naturally follows that the local equilibrium-distribution function for the chiral quasiparticles is captured by

$$\bar{\tilde{g}}_\chi = \delta\mu_\chi. \quad (21)$$

For the emergence of the longitudinal magnetoconductivity (LMC), it is necessary that the contribution from intraband scatterings is stronger than that from the interband scattering, implying that we must have $1/\tau \gg 1/\tau_G$. Under these conditions, the system first reaches local equilibrium through intraband scattering and, thereafter, achieves global equilibrium through interband scattering [76]. Thus, the $\tau \ll \tau_G$ regime allows us to safely approximate $\tilde{g}_s^\chi \simeq \bar{\tilde{g}}_\chi$ in $I_{\text{coll}}^{\text{inter}}$. Furthermore, the global conservation of the net electric charge gives us the constraint

$$\rho_\chi \delta\mu_\chi = -\rho_{-\chi} \delta\mu_{-\chi}. \quad (22)$$

Hence, we finally obtain

$$\frac{I_{\text{coll}}}{f_0'(\xi_s^\chi)} \simeq \frac{\tilde{g}_s^\chi(\mathbf{k}) - \delta\mu_\chi}{\tau} + \frac{\delta\mu_\chi - \delta\mu_{-\chi}}{2\tau_G} = \frac{\tilde{g}_s^\chi(\mathbf{k})}{\tau} - \frac{\delta\mu_\chi}{\tau} \left[1 - \frac{\tau}{2\tau_G} \left(1 + \frac{\rho_\chi}{\rho_{-\chi}} \right) \right]. \quad (23)$$

On including internode scatterings, the linearized Boltzmann equation, described in Eq. (11), gets modified to

$$\begin{aligned} e \mathcal{D}_s^\chi [\{\mathbf{w}_s^\chi + e(\boldsymbol{\Omega}_s^\chi \cdot \mathbf{w}_s^\chi) \mathbf{B}\} \cdot \mathbf{E}] - e \mathcal{D}_s^\chi \tilde{L} \tilde{g}_s^\chi(\mathbf{k}) &= -\frac{\tilde{g}_s^\chi(\mathbf{k})}{\tau} + \frac{\delta\mu_\chi}{\tau} \left[1 - \frac{\tau}{2\tau_G} \left(1 + \frac{\rho_\chi}{\rho_{-\chi}} \right) \right] \\ \Rightarrow (1 - e\tau \mathcal{D}_s^\chi \tilde{L}) \tilde{g}_s^\chi &= -e\tau \mathcal{D}_s^\chi [\{\mathbf{w}_s^\chi + e(\boldsymbol{\Omega}_s^\chi \cdot \mathbf{w}_s^\chi) \mathbf{B}\} \cdot \mathbf{E}] + \delta\mu_\chi \left[1 - \frac{\tau}{2\tau_G} \left(1 + \frac{\rho_\chi}{\rho_{-\chi}} \right) \right]. \end{aligned} \quad (24)$$

Using the fact that the application of \tilde{L} on the $\delta\mu_\chi$ -dependent term yields zero, Eq. (24) is rewritten as

$$\tilde{g}_s^\chi(\mathbf{k}) = -e\tau \sum_{n=0}^{\infty} (e\tau \mathcal{D}_s^\chi)^n \tilde{L}^n [\mathcal{D}_s^\chi \{\mathbf{w}_s^\chi + e(\boldsymbol{\Omega}_s^\chi \cdot \mathbf{w}_s^\chi) \mathbf{B}\} \cdot \mathbf{E}] + \delta\mu_\chi \left[1 - \frac{\tau}{2\tau_G} \left(1 + \frac{\rho_\chi}{\rho_{-\chi}} \right) \right]. \quad (25)$$

which we solve for $\tilde{g}_s^\chi(\mathbf{k})$ recursively. We can now expand the $\tilde{g}_s^\chi(\mathbf{k})$ upto any desired order in B , in the limit of weak magnetic field, and obtain the current densities. We observe that $\tilde{g}_s^\chi(\mathbf{k})$ consists of two parts, which are of different origins. The first part, which includes the classical effect due to the Lorentz force, is independent of $\delta\mu_\chi$. The second term, on the other hand, is proportional to $\delta\mu_\chi$ and goes to zero if the chemical potential at the two nodes are the same.

C. Conductivity arising from internode scatterings

The solution for $\tilde{g}_s^X(\mathbf{k})$ excluding the Lorentz-force part, is obtained from Eq. (25) by setting $n = 0$ in the summation on the RHS. In other words, we need to consider the equation

$$\tilde{g}_s^X(\mathbf{k}) = -e\tau \mathcal{D}_s^X \{ \mathbf{w}_s^X + e(\boldsymbol{\Omega}_s^X \cdot \mathbf{w}_s^X) \mathbf{B} \} \cdot \mathbf{E} + \delta\mu_\chi \left[1 - \frac{\tau}{2\tau_G} \left(1 + \frac{\rho_\chi}{\rho_{-\chi}} \right) \right]. \quad (26)$$

First, we need to determine $\delta\mu_\chi$ self-consistently by taking an average of both the sides of the above equation, which yields

$$\delta\mu_\chi \left[1 - \frac{\tau}{2\tau_G} \left(1 + \frac{\rho_\chi}{\rho_{-\chi}} \right) \right] = \bar{g}_\chi + e\tau \langle \mathcal{D}_s^X \{ \mathbf{w}_s^X + e(\boldsymbol{\Omega}_s^X \cdot \mathbf{w}_s^X) \mathbf{B} \} \cdot \mathbf{E} \rangle \Rightarrow \delta\mu_\chi = -\frac{2e\tau_G}{1 + \frac{\rho_\chi}{\rho_{-\chi}}} \frac{\mathcal{I}^X \cdot \mathbf{E}}{\rho_\chi}, \text{ where}$$

$$\mathcal{I}^X = \rho_\chi \langle \mathcal{D}_s^X \{ \mathbf{w}_s^X + e(\boldsymbol{\Omega}_s^X \cdot \mathbf{w}_s^X) \mathbf{B} \} \rangle = \sum_s \int \frac{d^3\mathbf{k}}{(2\pi)^3} [-f'_0(\xi_s^X(\mathbf{k}))] \{ \mathbf{w}_s^X + e(\boldsymbol{\Omega}_s^X \cdot \mathbf{w}_s^X) \mathbf{B} \}. \quad (27)$$

The non-anomalous-Hall contribution to the current, excluding the Lorentz-force part, is obtained by using Eqs. (17) and (26), leading to

$$\begin{aligned} \bar{\mathbf{J}}_s^X &= -e \int \frac{d^3\mathbf{k}}{(2\pi)^3} [-f'_0(\xi_s^X)] [\mathbf{w}_s^X + e(\boldsymbol{\Omega}_s^X \cdot \mathbf{w}_s^X) \mathbf{B}] \tilde{g}_s^X(\mathbf{k}) = \mathbf{J}_s^{X,\text{intra}} + \mathbf{J}_s^{X,\text{inter}}, \\ \mathbf{J}_s^{X,\text{intra}} &= e^2 \tau \int \frac{d^3\mathbf{k}}{(2\pi)^3} \mathcal{D}_s^X [-f'_0(\xi_s^X)] [\mathbf{w}_s^X + e(\boldsymbol{\Omega}_s^X \cdot \mathbf{w}_s^X) \mathbf{B}] \{ \mathbf{w}_s^X + e(\boldsymbol{\Omega}_s^X \cdot \mathbf{w}_s^X) \mathbf{B} \} \cdot \mathbf{E}, \\ \mathbf{J}_s^{X,\text{inter}} &= \frac{2e^2}{1 + \frac{\rho_\chi}{\rho_{-\chi}}} \left[\tau_G - \frac{\tau}{2} \left(1 + \frac{\rho_\chi}{\rho_{-\chi}} \right) \right] \int \frac{d^3\mathbf{k}}{(2\pi)^3} [-f'_0(\xi_s^X)] [\mathbf{w}_s^X + e(\boldsymbol{\Omega}_s^X \cdot \mathbf{w}_s^X) \mathbf{B}] \frac{\mathcal{I}^X \cdot \mathbf{E}}{\rho_\chi}. \end{aligned} \quad (28)$$

Therefore, the conductivity tensor, corresponding to the internode-scattering-induced current, is given by

$$(\sigma_s^{X,\text{inter}})_{ij} = \frac{e^2 \rho_{-\chi}}{\rho_\chi \rho_G} \left[\tau_G - \frac{\tau \rho_G}{\rho_{-\chi}} \right] \int \frac{d^3\mathbf{k}}{(2\pi)^3} [-f'_0(\xi_s^X)] [(w_s^X)_i + e(\boldsymbol{\Omega}_s^X \cdot \mathbf{w}_s^X) B_i] \mathcal{I}_j^X, \quad \rho_G = \frac{\rho_\chi + \rho_{-\chi}}{2}. \quad (29)$$

We show the expanded form of the integrand in Appendix A, retaining terms upto order B^2 . For the cases when ε_s^X is a function of magnitudes of the momentum components (i.e., $\varepsilon_s^X(\mathbf{k}) = \varepsilon_s^X(|k_x|, |k_y|, |k_z|)$), $f'_0(\varepsilon_s^X(\mathbf{k}))$ and its derivatives are even functions of \mathbf{k} . Since integrands which are odd functions of the momentum-components must vanish, we conclude that $\rho_\chi^{(1)} = I_j^{X,0} = \rho_G^{(1)} = I_j^{X,0} = \int \frac{d^3\mathbf{k}}{(2\pi)^3} \zeta_{0,ij}^{X,s} = \int \frac{d^3\mathbf{k}}{(2\pi)^3} \zeta_{1,ij}^{X,s} = 0$. This results in

$$\begin{aligned} (\sigma_s^{X,\text{inter}})_{ij} &= \frac{e^2 \left[\tau_G \rho_{-\chi}^{(0)} - \tau \rho_G^{(0)} \right] \Upsilon_i^{X,s} \mathcal{I}_j^{X,1}}{\rho_G^{(0)} \rho_\chi^{(0)}} B_i B_j + \mathcal{O}(B^2), \quad \rho_\chi^{(0)} = \sum_{\bar{s}} \int \frac{d^3\mathbf{q}}{(2\pi)^3} \{ -f'_0(\varepsilon_{\bar{s}}^X(\mathbf{q})) \}, \quad \rho_G^{(0)} = \frac{\rho_\chi^{(0)} + \rho_{-\chi}^{(0)}}{2}, \\ \mathcal{I}_j^{X,1} &= \sum_{\bar{s}} \Upsilon_j^{X,\bar{s}}, \quad \Upsilon_j^{X,s} = \int \frac{d^3\mathbf{k}}{(2\pi)^3} \left[e \boldsymbol{\Omega}_s^X(\mathbf{k}) \cdot \mathbf{v}_s^X(\mathbf{k}) \{ -f'_0(\varepsilon_s^X(\mathbf{k})) \} + (m_s^X(\mathbf{k}))_j (v_s^X(\mathbf{k}))_j f''_0(\varepsilon_s^X(\mathbf{k})) \right]. \end{aligned} \quad (30)$$

We note that the first nonzero term is of the order B^2 , which agrees with the results found in the literature [34, 71, 72] for the case of a pair of conjugate nodes for a WSM (harbouring the simplest case of twofold nodes). Needless to say that our formula of course applies to the generic cases of multifold nodes.

For the special case when we have scatterings between two nodes of the same nature, Eq. (30) further simplifies to

$$(\sigma_s^{X,\text{inter}})_{ij} = \frac{e^2 (\tau_G - \tau) B_i B_j}{\rho_1^{(0)}} \Upsilon_i^{1,s} \sum_{\bar{s}} \Upsilon_j^{1,\bar{s}}, \quad (31)$$

where we have used the fact that $s(\chi) = s(-\chi)$, $\varepsilon_s^X = \varepsilon_s^{-X} \equiv \varepsilon_s$, $\rho_\chi^{(0)} = \rho_{-\chi}^{(0)}$, $v_s^X = v_s^{-X}$, $\boldsymbol{\Omega}_s^X = -\boldsymbol{\Omega}_s^{-X}$, and $\mathbf{m}_s^X = -\mathbf{m}_s^{-X}$.

III. SPECIFIC EXAMPLES

Using the generic forms derived in Sec. II C, we now aim to derive the explicit expressions of the conductivity tensors embodying the chiral currents in specific systems. For the sake of simplicity, we will limit ourselves to the $T \rightarrow 0$ limit [such that $\{ -f'_0(\varepsilon_s^X(\mathbf{k})) \} \rightarrow \delta(E_F - \varepsilon_s^X(\mathbf{k}))$]. We consider the situations when both $\mu_\chi > 0$ and $\mu_{-\chi} > 0$, such that the chiral quiparticles occupying the positive-energy bands participate in transport. For all the Hamiltonians shown below, v_0 denotes the effective Fermi velocity for the isotropic and linearly dispersing bands. In order to carry out the integrations, taking advantage of the isotropy of the systems that we consider here, we resort to the spherical polar coordinates (as shown in Appendix B).

A. Weyl semimetal

A single node of a WSM, with chirality χ , is represented by

$$\mathcal{H}_{\text{WSM}}(\mathbf{k}) = v_0 (k_x \sigma_x + k_y \sigma_y + \chi k_z \sigma_z), \quad (32)$$

where $\boldsymbol{\sigma} = \{\sigma_x, \sigma_y, \sigma_z\}$ represents the vector operator comprising the three Pauli matrices. The dispersion relations of the two bands meeting at the nodal point are given by

$$\varepsilon_s^{\text{WSM}}(k) = s v_0 k, \quad s = \pm 1, \quad (33)$$

where $k = \sqrt{k_x^2 + k_y^2 + k_z^2}$. The corresponding group velocities of the quasiparticles are given by

$$\mathbf{v}_s^{\text{WSM}}(\mathbf{k}) = \nabla_{\mathbf{k}} \varepsilon_s^{\text{WSM}}(\mathbf{k}) = \frac{s v_0 \mathbf{k}}{k}. \quad (34)$$

The BC and the OMM are captured by the following expressions:

$$\boldsymbol{\Omega}_s^\chi(\mathbf{k}) = -\frac{\chi s \mathbf{k}}{2 k^3} \text{ and } \mathbf{m}_s^\chi(\mathbf{k}) = -\frac{e \chi v_0 \mathbf{k}}{2 k^2}. \quad (35)$$

Using Eq. (31), the internode-scattering-induced conductivity components, considering a pair of conjugate Weyl nodes, thus reduces to the simple form of

$$\left(\sigma_1^{\chi, \text{inter}}\right)_{ij} = \frac{2 e^4 v_0^3 (\tau_G - \tau) B_i B_j}{9 \pi^2 E_F^2}. \quad (36)$$

B. Triple-point semimetal

A single node of a TSM, with chirality χ , is represented by

$$\mathcal{H}_{\text{TSM}}(\mathbf{k}) = v_0 (k_x \mathcal{S}_x + k_y \mathcal{S}_y + \chi k_z \mathcal{S}_z), \quad (37)$$

where $\boldsymbol{\mathcal{S}} = \{\mathcal{S}_x, \mathcal{S}_y, \mathcal{S}_z\}$ represents the vector operator in the spin-1 representation. We choose

$$\mathcal{S}_x = \frac{1}{\sqrt{2}} \begin{pmatrix} 0 & 1 & 0 \\ 1 & 0 & 1 \\ 0 & 1 & 0 \end{pmatrix}, \quad \mathcal{S}_y = \frac{1}{\sqrt{2}} \begin{pmatrix} 0 & -i & 0 \\ i & 0 & -i \\ 0 & i & 0 \end{pmatrix}, \quad \mathcal{S}_z = \begin{pmatrix} 1 & 0 & 0 \\ 0 & 0 & 0 \\ 0 & 0 & -1 \end{pmatrix}. \quad (38)$$

The energy eigenvalues, group velocities, BC, and OMM are obtained in the following forms:

$$\begin{aligned} \varepsilon_s^{\text{TRM}}(k) &= s v_0 k \text{ and } \mathbf{v}_s^{\text{TRM}}(\mathbf{k}) = \nabla_{\mathbf{k}} \varepsilon_s(\mathbf{k}) = \frac{s v_0 \mathbf{k}}{k}, \text{ where } s \in \{\pm 1, 0\}; \\ \boldsymbol{\Omega}_s^\chi(\mathbf{k}) &= -\frac{\chi s \mathbf{k}}{k^3} \text{ and } \mathbf{m}_s^\chi(\mathbf{k}) = -\frac{e \chi v_0 \mathcal{G}_s \mathbf{k}}{2 k^2}, \text{ where } \{\mathcal{G}_{\pm 1}, \mathcal{G}_0\} = \{1, 2\}. \end{aligned} \quad (39)$$

For the internode-scattering-induced conductivity components, arising from a pair of conjugate nodes of a TSM [4, 11], Eq. (31) gives us

$$\left(\sigma_1^{\chi, \text{inter}}\right)_{ij} = \frac{49 e^4 v_0^3 (\tau_G - \tau) B_i B_j}{72 \pi^2 E_F^2}. \quad (40)$$

We would like to point out that the overall numerical factor differs from that of the WSM case [cf. Eq. (36)], which is expected, because the BC vector differs by a factor of two.

For the case depicted in Fig. 1, let us consider the internode-induced conductivity for the chiral quasiparticles at the TSM node with $\chi = 1$ (occupying the band $s = 1$). Then, Eq. (29) leads to

$$\left(\sigma_1^{1, \text{inter}}\right)_{ij} = \frac{49 e^4 v_0^3 \left[\tau_G - \frac{\tau}{4} \left\{ 2 + \left(\frac{\tilde{v}_0}{v_0} \right)^3 \right\} \right] B_i B_j}{18 \pi^2 E_F^2 \left\{ 2 + \left(\frac{\tilde{v}_0}{v_0} \right)^3 \right\}}, \quad (41)$$

where v_0 and \tilde{v}_0 denote the group velocities of the pseudospin-1 (for TSM) and pseudospin-1/2 (for WSM) quasiparticles, respectively.

C. Rarita-Schwinger-Weyl semimetal

The explicit form of the Hamiltonian for a single RSW node with chirality χ is given by

$$\mathcal{H}_{\text{RSW}}(\mathbf{k}) = v_0 (k_x \mathcal{J}_x + k_y \mathcal{J}_y + \chi k_z \mathcal{J}_z), \quad (42)$$

where $\mathcal{J} = \{\mathcal{J}_x, \mathcal{J}_y, \mathcal{J}_z\}$ represents the vector operator whose three components comprise the the angular momentum operators in the spin-3/2 representation of the SU(2) group. We choose the commonly-used representation where

$$\mathcal{J}_x = \begin{pmatrix} 0 & \frac{\sqrt{3}}{2} & 0 & 0 \\ \frac{\sqrt{3}}{2} & 0 & 1 & 0 \\ 0 & 1 & 0 & \frac{\sqrt{3}}{2} \\ 0 & 0 & \frac{\sqrt{3}}{2} & 0 \end{pmatrix}, \quad \mathcal{J}_y = \begin{pmatrix} 0 & \frac{-i\sqrt{3}}{2} & 0 & 0 \\ \frac{i\sqrt{3}}{2} & 0 & -i & 0 \\ 0 & i & 0 & \frac{-i\sqrt{3}}{2} \\ 0 & 0 & \frac{i\sqrt{3}}{2} & 0 \end{pmatrix}, \quad \mathcal{J}_z = \begin{pmatrix} \frac{3}{2} & 0 & 0 & 0 \\ 0 & \frac{1}{2} & 0 & 0 \\ 0 & 0 & -\frac{1}{2} & 0 \\ 0 & 0 & 0 & -\frac{3}{2} \end{pmatrix}. \quad (43)$$

The energy eigenvalues, group velocities, BC, and OMM are obtained are found to be:

$$\begin{aligned} \varepsilon_s^{\text{RSW}}(k) &= s v_0 k \text{ and } \mathbf{v}_s^{\text{RSW}}(\mathbf{k}) = \nabla_{\mathbf{k}} \varepsilon_s(\mathbf{k}) = \frac{s v_0 \mathbf{k}}{k}, \text{ where } s \in \left\{ \pm \frac{1}{2}, \pm \frac{3}{2} \right\}; \\ \boldsymbol{\Omega}_s^{\chi}(\mathbf{k}) &= -\frac{\chi s \mathbf{k}}{k^3} \text{ and } \mathbf{m}_s^{\chi}(\mathbf{k}) = -\frac{e \chi v_0 \mathcal{G}_s \mathbf{k}}{k^2}, \text{ where } \{\mathcal{G}_{\pm 1/2}, \mathcal{G}_{\pm 3/2}\} = \left\{ \frac{7}{4}, \frac{3}{4} \right\}. \end{aligned} \quad (44)$$

For the case depicted in Fig. 2, let us consider the internode-induced conductivity for the chiral quasiparticles at the RSW node with $\chi = 1$. Then, Eq. (29) leads to

$$\left(\sigma_{1/2}^{1,\text{inter}} \right)_{ij} = \left(\sigma_{3/2}^{1,\text{inter}} \right)_{ij} = \frac{285 e^4 v_0^3 \left[27 \tau_G - \frac{\tau}{2} \left\{ 27 + 112 \left(\frac{\tilde{v}_0}{v_0} \right)^3 \right\} \right]}{448 \pi^2 E_F^2 \left\{ 27 + 112 \left(\frac{\tilde{v}_0}{v_0} \right)^3 \right\}} \quad (45)$$

for both the bands with $s = 1/2$ and $s = 3/2$. Here, v_0 and \tilde{v}_0 denote the group velocities of the pseudospin-3/2 (for the RSW node) and pseudospin-1 (for TSM) quasiparticles, respectively.

IV. SUMMARY AND FUTURE PERSPECTIVES

In this paper, we have derived a generic expression for the components of the chiral conductivity when we have multifold band-degeneracies. Since the sum of all the monopole charges in the BZ are constrained to vanish, the nodes appear in pairs of $\chi = \pm 1$. Consequently, the presence of band-crossing degeneracies of order higher than two provide a richer playground — the pair of conjugate nodes in question are comprised of bands which can be of the same pseudospin variety, or can carry quantum numbers of two distinct pseudospin-representations. Covering both these two possibilities, we have applied our derived formula to chiral crystals which harbour nodes of the TSM and RSW varieties, thus showing the explicit final expressions of the components of the chiral-conductivity tensor. In our computations, we have accounted for the effects of both the BC and the OMM, thus covering all the topologically-induced modifications in the derivation leading to the linearized Boltzmann equations. We would like to emphasize that since we have used the methodology based on the relaxation-time approximation, in the future, it will be worthwhile to derive the chiral linear response by going beyond the phenomenological approximations of the relaxation processes [44]. Due to various contemporary experiments exploring the conductivity of multifold fermions [8], we expect these theoretical studies to contribute towards a deeper understanding of semimetals with nontrivial topology in their bandstructures.

ACKNOWLEDGMENTS

We thank Firdous Haidar for useful discussions.

Appendix A: Terms expanded upto order B^2

In this appendix, we expand the integrand of Eq. (29) by keeping terms upto order B^2 . For this purpose, we define

$$\begin{aligned}
\rho_\chi &= \rho_\chi^{(0)} + \rho_\chi^{(1)} + \rho_\chi^{(2)} + \mathcal{O}(B^3), \\
&= \sum_s \int \frac{d^3 \mathbf{q}}{(2\pi)^3} \{-f'_0(\varepsilon_s^\chi(\mathbf{q}))\}, \quad \rho_\chi^{(1)} = \sum_s \int \frac{d^3 \mathbf{q}}{(2\pi)^3} [e \mathbf{B} \cdot \boldsymbol{\Omega}_s^\chi(\mathbf{q}) \{-f'_0(\varepsilon_s^\chi(\mathbf{q}))\} + \eta_s^\chi(\mathbf{q}) \{-f''_0(\varepsilon_s^\chi(\mathbf{q}))\}], \\
\rho_\chi^{(2)} &= \sum_s \int \frac{d^3 \mathbf{q}}{(2\pi)^3} \eta_s^\chi(\mathbf{q}) \left[e \mathbf{B} \cdot \boldsymbol{\Omega}_s^\chi(\mathbf{q}) \{-f''_0(\varepsilon_s^\chi(\mathbf{q}))\} + \frac{\{\eta_s^\chi(\mathbf{q})\}^2}{2} \{-f'''_0(\varepsilon_s^\chi(\mathbf{q}))\} \right], \tag{A1}
\end{aligned}$$

$$\rho_G = \rho_G^{(0)} + \rho_G^{(1)} + \rho_G^{(2)} + \mathcal{O}(B^3), \quad \rho_G^{(0)} = \frac{\rho_\chi^{(0)} + \rho_{-\chi}^{(0)}}{2}, \quad \rho_G^{(1)} = \frac{\rho_\chi^{(1)} + \rho_{-\chi}^{(1)}}{2}, \quad \rho_G^{(2)} = \frac{\rho_\chi^{(2)} + \rho_{-\chi}^{(2)}}{2}, \tag{A2}$$

$$\begin{aligned}
\mathcal{I}_j^\chi &= \mathcal{I}_j^{\chi,0} + \mathcal{I}_j^{\chi,1} + \mathcal{I}_j^{\chi,2} + \mathcal{O}(B^3), \\
\mathcal{I}_j^{\chi,0} &= \sum_s \int \frac{d^3 \mathbf{q}}{(2\pi)^3} (v_s^\chi(\mathbf{q}))_j \{-f'_0(\varepsilon_s^\chi(\mathbf{q}))\}, \\
\mathcal{I}_j^{\chi,1} &= \sum_s \int \frac{d^3 \mathbf{q}}{(2\pi)^3} \left[\{e \boldsymbol{\Omega}_s^\chi(\mathbf{q}) \cdot \mathbf{v}_s^\chi(\mathbf{q}) B_j + (u_s^\chi(\mathbf{q}))_j\} \{-f'_0(\varepsilon_s^\chi(\mathbf{q}))\} + \eta_s^\chi(\mathbf{q}) (v_s(\mathbf{q}))_j \{-f''_0(\varepsilon_s^\chi(\mathbf{q}))\} \right], \\
\mathcal{I}_j^{\chi,2} &= \sum_s \int \frac{d^3 \mathbf{q}}{(2\pi)^3} \left[e \boldsymbol{\Omega}_s^\chi(\mathbf{q}) \cdot \mathbf{u}_s^\chi(\mathbf{q}) B_j \{-f'_0(\varepsilon_s^\chi(\mathbf{q}))\} + \eta_s^\chi(\mathbf{q}) \{e \boldsymbol{\Omega}_s^\chi(\mathbf{q}) \cdot \mathbf{v}_s^\chi(\mathbf{q}) B_j + (u_s^\chi(\mathbf{q}))_j\} \{-f''_0(\varepsilon_s^\chi(\mathbf{q}))\} \right. \\
&\quad \left. + \frac{(\eta_s^\chi(\mathbf{q}))^2 (v_s^\chi(\mathbf{q}))_j}{2} \{-f'''_0(\varepsilon_s^\chi(\mathbf{q}))\} \right]. \tag{A3}
\end{aligned}$$

This leads to

$$(\sigma_s^{\chi, \text{inter}})_{ij} = \frac{e^2 [\tau \rho_G^{(0)} - \tau_G \rho_{-\chi}^{(0)}]}{\rho_G^{(0)} \rho_\chi^{(0)}} \int \frac{d^3 \mathbf{k}}{(2\pi)^3} \left[\varsigma_{0,ij}^{\chi,s} + \varsigma_{1,ij}^{\chi,s} + \frac{\varsigma_{2,ij}^{\chi,s}}{\{\rho_G^{(0)} \rho_\chi^{(0)}\}^2} \right] + \mathcal{O}(B^2), \tag{A4}$$

where

$$\varsigma_{0,ij}^{\chi,s}(\mathbf{k}) = -\mathcal{I}_j^{\chi,0} (v_s^\chi)_i, \tag{A5}$$

$$\begin{aligned}
\varsigma_{1,ij}^{\chi,s}(\mathbf{k}) &= \left[\left[-e \boldsymbol{\Omega}_s^\chi \cdot \mathbf{v}_s^\chi B_i + \left\{ \frac{\tau_G}{\rho_G^{(0)}} \frac{\rho_G^{(0)} \rho_{-\chi}^{(1)} - \rho_G^{(1)} \rho_{-\chi}^{(0)}}{\tau \rho_G^{(0)} - \tau_G \rho_{-\chi}^{(0)}} + \frac{\rho_\chi^{(1)}}{\rho_\chi^{(0)}} \right\} (v_s^\chi)_i - (u_s^\chi)_i \right] \mathcal{I}_j^{\chi,0} - (v_s^\chi)_i \mathcal{I}_j^{\chi,1} \right] \{-f'_0(\varepsilon_s^\chi)\} \\
&\quad - \eta_s^\chi (v_s^\chi)_i \mathcal{I}_j^{\chi,0} \{-f''_0(\varepsilon_s^\chi)\}, \tag{A6}
\end{aligned}$$

$$\begin{aligned}
\varsigma_{2,ij}^{\chi,s}(\mathbf{k}) = & \left[e \rho_G^{(0)} \rho_\chi^{(0)} \boldsymbol{\Omega}_s^\chi \cdot \mathbf{v}_s^\chi \left\{ \tau \rho_G^{(0)} \left(\tau_G \rho_\chi^{(0)} \rho_{-\chi}^{(1)} + \tau \rho_G^{(0)} \rho_\chi^{(1)} \right) - \tau_G \rho_{-\chi}^{(0)} \left(\rho_G^{(1)} \rho_\chi^{(0)} + \rho_G^{(0)} \rho_\chi^{(1)} \right) \right\} B_i \right. \\
& + e \left(\rho_G^{(0)} \rho_\chi^{(0)} \right)^2 \boldsymbol{\Omega}_s^\chi \cdot \mathbf{u}_s^\chi \left(\tau_G \rho_{-\chi}^{(0)} - \tau \rho_G^{(0)} \right) B_i - \tau_G \rho_{-\chi}^{(0)} \rho_G^{(0)} \rho_\chi^{(0)} \left\{ \rho_G^{(1)} \rho_\chi^{(0)} - \rho_G^{(0)} \rho_\chi^{(1)} \right\} (u_s^\chi)_i + \tau_G \left(\rho_G^{(0)} \rho_\chi^{(0)} \right)^2 \rho_{-\chi}^{(1)} (u_s^\chi)_i \\
& + \tau \left(\rho_G^{(0)} \right)^3 \rho_\chi^{(0)} \rho_\chi^{(1)} (u_s^\chi)_i + \tau_G \rho_{-\chi}^{(0)} \left(\rho_G^{(1)} \right)^2 \left(\rho_\chi^{(0)} \right)^2 (v_s^\chi)_i + \tau_G \rho_{-\chi}^{(0)} \left(\rho_G^{(0)} \right)^2 \left(\rho_\chi^{(1)} \right)^2 (v_s^\chi)_i + \tau_G \rho_{-\chi}^{(0)} \rho_G^{(0)} \rho_G^{(1)} \rho_\chi^{(0)} \rho_\chi^{(1)} (v_s^\chi)_i \\
& - \tau_G \rho_G^{(0)} \rho_G^{(1)} \left(\rho_\chi^{(0)} \right)^2 \rho_{-\chi}^{(1)} (v_s^\chi)_i - \tau \left(\rho_G^{(0)} \right)^3 \left(\rho_\chi^{(1)} \right)^2 (v_s^\chi)_i - \tau_G \left(\rho_G^{(0)} \right)^2 \rho_\chi^{(0)} \rho_{-\chi}^{(1)} \rho_\chi^{(1)} (v_s^\chi)_i - \tau_G \rho_G^{(2)} \rho_{-\chi}^{(0)} \rho_G^{(0)} \left(\rho_\chi^{(0)} \right)^2 (v_s^\chi)_i \\
& \left. + \tau_G \rho_{-\chi}^{(2)} \left(\rho_G^{(0)} \right)^2 \left(\rho_\chi^{(0)} \right)^2 (v_s^\chi)_i + \rho_\chi^{(2)} \left(\rho_G^{(0)} \right)^2 \rho_\chi^{(0)} \left(\tau \rho_G^{(0)} - \tau_G \rho_{-\chi}^{(0)} \right) (v_s^\chi)_i \right] \frac{\mathcal{I}_j^{\chi,0} \{-f_0'(\varepsilon_s^\chi)\}}{\left(\rho_G^{(0)} \rho_\chi^{(0)} \right)^2 \left[\tau \rho_G^{(0)} - \tau_G \rho_{-\chi}^{(0)} \right]} \\
& + \left[-e \boldsymbol{\Omega}_s^\chi \cdot \mathbf{v}_s^\chi B_i - (u_s^\chi)_i + \left\{ \frac{\tau_G}{\rho_G^{(0)}} \frac{\rho_G^{(0)} \rho_{-\chi}^{(1)} - \rho_{-\chi}^{(0)} \rho_G^{(1)}}{\tau \rho_G^{(0)} - \tau_G \rho_{-\chi}^{(0)}} + \frac{\rho_\chi^{(1)}}{\rho_\chi^{(0)}} \right\} (v_s^\chi)_i \right] \mathcal{I}_j^{\chi,1} \{-f_0'(\varepsilon_s^\chi)\} - (v_s^\chi)_i \mathcal{I}_j^{\chi,2} \{-f_0'(\varepsilon_s^\chi)\} \\
& + \eta_s^\chi \left[\left[-e \boldsymbol{\Omega}_s^\chi \cdot \mathbf{v}_s^\chi B_i - (u_s^\chi)_i + \left\{ \frac{\tau_G}{\rho_G^{(0)}} \frac{\rho_G^{(0)} \rho_{-\chi}^{(1)} - \rho_{-\chi}^{(0)} \rho_G^{(1)}}{\tau \rho_G^{(0)} - \tau_G \rho_{-\chi}^{(0)}} + \frac{\rho_\chi^{(1)}}{\rho_\chi^{(0)}} \right\} (v_s^\chi)_i \right] \mathcal{I}_j^{\chi,0} - (v_s^\chi)_i \mathcal{I}_j^{\chi,1} \right] \{-f_0''(\varepsilon_s^\chi)\} \\
& - \frac{(\eta_s^\chi)^2 (v_s^\chi)_i \mathcal{I}_j^{\chi,0}}{2} \{-f_0'''(\varepsilon_s^\chi)\}. \tag{A7}
\end{aligned}$$

In the last three equations, we have suppressed the \mathbf{k} -dependence of the various quantities.

Appendix B: Useful integrals

In the main text, we have to deal with integrals of the form:

$$\mathcal{I} = \int \frac{d^3 \mathbf{k}}{(2\pi)^3} F(\mathbf{k}, \varepsilon_s) f_0'(\varepsilon_s), \text{ where } \varepsilon_s = s v_0 k. \tag{B1}$$

Clearly, it is convenient to switch to the spherical polar coordinates using the standard transformations comprising

$$k_x = \frac{\tilde{\varepsilon} \cos \phi \sin \theta}{s v_0}, \quad k_y = \frac{\tilde{\varepsilon} \sin \phi \sin \theta}{s v_0}, \quad k_z = \frac{\tilde{\varepsilon} \cos \theta}{s v_0}, \tag{B2}$$

where $\tilde{\varepsilon} \in [0, \infty)$, $\phi \in [0, 2\pi)$, and $\theta \in [0, \pi]$. The Jacobian of the transformation is $\mathcal{J}(\tilde{\varepsilon}, \theta) = \frac{\tilde{\varepsilon}^2 \sin \theta}{s^3 v_0^3}$. This leads to

$$\int_{-\infty}^{\infty} d^3 \mathbf{k} \rightarrow \int_0^{\infty} d\tilde{\varepsilon} \int_0^{2\pi} d\phi \int_0^\pi d\theta \mathcal{J}(\tilde{\varepsilon}, \theta) \text{ and } \varepsilon_s(\mathbf{k}) \rightarrow \tilde{\varepsilon}, \tag{B3}$$

Since the dispersion does not depend on θ or ϕ , we can immediately perform the angular integrals as the first step, which makes many terms disappear.

-
- [1] A. A. Burkov and L. Balents, Weyl semimetal in a topological insulator multilayer, *Phys. Rev. Lett.* **107**, 127205 (2011).
 - [2] B. Yan and C. Felser, Topological materials: Weyl semimetals, *Annual Rev. of Condensed Matter Phys.* **8**, 337 (2017).
 - [3] I. Mandal and K. Saha, Thermoelectric response in nodal-point semimetals, *Annalen der Physik* **536**, 2400016 (2024).
 - [4] B. Bradlyn, J. Cano, Z. Wang, M. G. Vergniory, C. Felser, R. J. Cava, and B. A. Bernevig, Beyond Dirac and Weyl fermions: Unconventional quasiparticles in conventional crystals, *Science* **353** (2016).
 - [5] I. Mandal, Robust marginal Fermi liquid in birefringent semimetals, *Phys. Lett. A* **418**, 127707 (2021).
 - [6] F. Flicker, F. de Juan, B. Bradlyn, T. Morimoto, M. G. Vergniory, and A. G. Grushin, Chiral optical response of multifold fermions, *Phys. Rev. B* **98**, 155145 (2018).
 - [7] I. Mandal and H. Freire, Transport properties in non-Fermi liquid phases of nodal-point semimetals, *Journal of Physics: Condensed Matter* **36**, 443002 (2024).
 - [8] F. Balduini, A. Molinari, L. Rocchino, V. Hasse, C. Felser, M. Sousa, C. Zota, H. Schmid, A. G. Grushin, and B. Gotsmann, Intrinsic negative magnetoresistance from the chiral anomaly of multifold fermions, *Nature Communications* **15**, 6526 (2024).
 - [9] N. P. Armitage, E. J. Mele, and A. Vishwanath, Weyl and Dirac semimetals in three-dimensional solids, *Rev. Mod. Phys.* **90**, 015001 (2018).

- [10] I. Mandal, Transmission in pseudospin-1 and pseudospin-3/2 semimetals with linear dispersion through scalar and vector potential barriers, *Phys. Lett. A* **384**, 126666 (2020).
- [11] I. C. Fulga and A. Stern, Triple point fermions in a minimal symmorphic model, *Phys. Rev. B* **95**, 241116 (2017).
- [12] S. Nandy, K. Sengupta, and D. Sen, Transport across junctions of pseudospin-one fermions, *Phys. Rev. B* **100**, 085134 (2019).
- [13] S. Sekh and I. Mandal, Circular dichroism as a probe for topology in three-dimensional semimetals, *Phys. Rev. B* **105**, 235403 (2022).
- [14] P. Tang, Q. Zhou, and S.-C. Zhang, Multiple types of topological fermions in transition metal silicides, *Phys. Rev. Lett.* **119**, 206402 (2017).
- [15] Y. Shen, Y. Jin, Y. Ge, M. Chen, and Z. Zhu, Chiral topological metals with multiple types of quasiparticle fermions and large spin Hall effect in the SrGePt family materials, *Phys. Rev. B* **108**, 035428 (2023).
- [16] I. Mandal, Nature of Andreev bound states in Josephson junctions of triple-point semimetals, *arXiv e-prints* (2024), [arXiv:2406.15350 \[cond-mat.supr-con\]](https://arxiv.org/abs/2406.15350).
- [17] L. Liang and Y. Yu, Semimetal with both Rarita-Schwinger-Weyl and Weyl excitations, *Phys. Rev. B* **93**, 045113 (2016).
- [18] I. Boettcher, Interplay of topology and electron-electron interactions in Rarita-Schwinger-Weyl semimetals, *Phys. Rev. Lett.* **124**, 127602 (2020).
- [19] J. M. Link, I. Boettcher, and I. F. Herbut, d -wave superconductivity and Bogoliubov-Fermi surfaces in Rarita-Schwinger-Weyl semimetals, *Phys. Rev. B* **101**, 184503 (2020).
- [20] H. Isobe and L. Fu, Quantum critical points of $j = \frac{3}{2}$ Dirac electrons in antiperovskite topological crystalline insulators, *Phys. Rev. B* **93**, 241113 (2016).
- [21] J.-Z. Ma, Q.-S. Wu, M. Song, S.-N. Zhang, E. Guedes, S. Ekahana, M. Krivenkov, M. Yao, S.-Y. Gao, W.-H. Fan, *et al.*, Observation of a singular Weyl point surrounded by charged nodal walls in ptga, *Nature Communications* **12**, 3994 (2021).
- [22] Sekh, Sajid and Mandal, Ipsita, Magnus Hall effect in three-dimensional topological semimetals, *Eur. Phys. J. Plus* **137**, 736 (2022).
- [23] I. Mandal, Transmission and conductance across junctions of isotropic and anisotropic three-dimensional semimetals, *Eur. Phys. J. Plus* **138**, 1039 (2023).
- [24] I. Mandal, Andreev bound states in superconductor-barrier-superconductor junctions of Rarita-Schwinger-Weyl semimetals, *Phys. Lett. A* **503**, 129410 (2024).
- [25] R. Ghosh, F. Haidar, and I. Mandal, Linear response in planar Hall and thermal Hall setups for Rarita-Schwinger-Weyl semimetals, *arXiv e-prints* (2024), [arXiv:2408.01422 \[cond-mat.mes-hall\]](https://arxiv.org/abs/2408.01422).
- [26] I. Mandal, S. Saha, and R. Ghosh, Signatures of topology in generic transport measurements for Rarita-Schwinger-Weyl semimetals, *arXiv e-prints* (2024), [arXiv:2408.17447 \[cond-mat.mes-hall\]](https://arxiv.org/abs/2408.17447).
- [27] F. D. M. Haldane, Berry curvature on the Fermi surface: Anomalous Hall effect as a topological Fermi-liquid property, *Phys. Rev. Lett.* **93**, 206602 (2004).
- [28] P. Goswami and S. Tewari, Axionic field theory of $(3 + 1)$ -dimensional Weyl semimetals, *Phys. Rev. B* **88**, 245107 (2013).
- [29] A. A. Burkov, Anomalous Hall effect in Weyl metals, *Phys. Rev. Lett.* **113**, 187202 (2014).
- [30] S.-B. Zhang, H.-Z. Lu, and S.-Q. Shen, Linear magnetoconductivity in an intrinsic topological Weyl semimetal, *New Journal of Phys.* **18**, 053039 (2016).
- [31] Q. Chen and G. A. Fiete, Thermoelectric transport in double-Weyl semimetals, *Phys. Rev. B* **93**, 155125 (2016).
- [32] S. Nandy, G. Sharma, A. Taraphder, and S. Tewari, Chiral anomaly as the origin of the planar Hall effect in Weyl semimetals, *Phys. Rev. Lett.* **119**, 176804 (2017).
- [33] S. Nandy, A. Taraphder, and S. Tewari, Berry phase theory of planar Hall effect in topological insulators, *Scientific Reports* **8**, 14983 (2018).
- [34] K. Das and A. Agarwal, Linear magnetochiral transport in tilted type-I and type-II Weyl semimetals, *Phys. Rev. B* **99**, 085405 (2019).
- [35] K. Das and A. Agarwal, Thermal and gravitational chiral anomaly induced magneto-transport in Weyl semimetals, *Phys. Rev. Res.* **2**, 013088 (2020).
- [36] S. Das, K. Das, and A. Agarwal, Nonlinear magnetoconductivity in Weyl and multi-Weyl semimetals in quantizing magnetic field, *Phys. Rev. B* **105**, 235408 (2022).
- [37] O. Pal, B. Dey, and T. K. Ghosh, Berry curvature induced magnetotransport in 3D noncentrosymmetric metals, *Journal of Phys.: Condensed Matter* **34**, 025702 (2022).
- [38] O. Pal, B. Dey, and T. K. Ghosh, Berry curvature induced anisotropic magnetotransport in a quadratic triple-component fermionic system, *Journal of Phys.: Condensed Matter* **34**, 155702 (2022).
- [39] L. X. Fu and C. M. Wang, Thermoelectric transport of multi-Weyl semimetals in the quantum limit, *Phys. Rev. B* **105**, 035201 (2022).
- [40] Y. Araki, Magnetic Textures and Dynamics in Magnetic Weyl Semimetals, *Annalen der Physik* **532**, 1900287 (2020).
- [41] Y. P. Mizuta and F. Ishii, Contribution of Berry curvature to thermoelectric effects, *Proceedings of the International Conference on Strongly Correlated Electron Systems (SCES2013)*, *JPS Conf. Proc.* **3**, 017035 (2014).
- [42] S. Yadav, S. Fazzini, and I. Mandal, Magneto-transport signatures in periodically-driven Weyl and multi-Weyl semimetals, *Physica E Low-Dimensional Systems and Nanostructures* **144**, 115444 (2022).
- [43] R. Ghosh and I. Mandal, Electric and thermoelectric response for Weyl and multi-Weyl semimetals in planar Hall configurations including the effects of strain, *Physica E: Low-dimensional Systems and Nanostructures* **159**, 115914 (2024).
- [44] A. Knoll, C. Timm, and T. Meng, Negative longitudinal magnetoconductance at weak fields in Weyl semimetals, *Phys. Rev. B* **101**, 201402 (2020).
- [45] R. Ghosh and I. Mandal, Direction-dependent conductivity in planar Hall set-ups with tilted Weyl/multi-Weyl semimetals, *Journal of Physics: Condensed Matter* **36**, 275501 (2024).
- [46] L. Medel, R. Ghosh, A. Martín-Ruiz, and I. Mandal, Electric, thermal, and thermoelectric magnetoconductivity for Weyl/multi-Weyl semimetals in planar Hall set-ups induced by the combined effects of topology and strain, *Scientific Reports* **14**, 21390 (2024).

- [47] I. Mandal, Anisotropic conductivity for the type-I and type-II phases of Weyl/multi-Weyl semimetals in planar Hall set-ups, [arXiv e-prints \(2024\)](#), [arXiv:2410.05028 \[cond-mat.mes-hall\]](#).
- [48] V. Gusynin, S. Sharapov, and J. Carbotte, Magneto-optical conductivity in graphene, [Journal of Phys.: Condensed Matter](#) **19**, 026222 (2006).
- [49] M. Stålhammar, J. Larana-Aragon, J. Knolle, and E. J. Bergholtz, Magneto-optical conductivity in generic Weyl semimetals, [Phys. Rev. B](#) **102**, 235134 (2020).
- [50] S. Yadav, S. Sekh, and I. Mandal, Magneto-optical conductivity in the type-I and type-II phases of Weyl/multi-Weyl semimetals, [Physica B: Condensed Matter](#) **656**, 414765 (2023).
- [51] M. Papaj and L. Fu, Magnus Hall effect, [Phys. Rev. Lett.](#) **123**, 216802 (2019).
- [52] D. Mandal, K. Das, and A. Agarwal, Magnus Nernst and thermal Hall effect, [Phys. Rev. B](#) **102**, 205414 (2020).
- [53] I. Mandal, Signatures of two- and three-dimensional semimetals from circular dichroism, [International Journal of Modern Physics B](#) **38**, 2450216 (2024).
- [54] J. E. Moore, Optical properties of Weyl semimetals, [National Science Rev.](#) **6**, 206 (2018).
- [55] C. Guo, V. S. Asadchy, B. Zhao, and S. Fan, Light control with Weyl semimetals, [eLight](#) **3**, 2 (2023).
- [56] A. Avdoshkin, V. Kozii, and J. E. Moore, Interactions remove the quantization of the chiral photocurrent at Weyl points, [Phys. Rev. Lett.](#) **124**, 196603 (2020).
- [57] I. Mandal, Effect of interactions on the quantization of the chiral photocurrent for double-Weyl semimetals, [Symmetry](#) **12** (2020).
- [58] I. Mandal and A. Sen, Tunneling of multi-Weyl semimetals through a potential barrier under the influence of magnetic fields, [Phys. Lett. A](#) **399**, 127293 (2021).
- [59] S. Bera and I. Mandal, Floquet scattering of quadratic band-touching semimetals through a time-periodic potential well, [Journal of Phys. Condensed Matter](#) **33**, 295502 (2021).
- [60] S. Bera, S. Sekh, and I. Mandal, Floquet transmission in Weyl/multi-Weyl and nodal-line semimetals through a time-periodic potential well, [Ann. Phys. \(Berlin\)](#) **535**, 2200460 (2023).
- [61] D. Xiao, M.-C. Chang, and Q. Niu, Berry phase effects on electronic properties, [Rev. Mod. Phys.](#) **82**, 1959 (2010).
- [62] G. Sundaram and Q. Niu, Wave-packet dynamics in slowly perturbed crystals: Gradient corrections and Berry-phase effects, [Phys. Rev. B](#) **59**, 14915 (1999).
- [63] A. Graf and F. Piéchon, Berry curvature and quantum metric in N -band systems: An eigenprojector approach, [Phys. Rev. B](#) **104**, 085114 (2021).
- [64] J. Cayssol and J. N. Fuchs, Topological and geometrical aspects of band theory, [Journal of Physics: Materials](#) **4**, 034007 (2021).
- [65] M. M. H. Polash, S. Yalameha, H. Zhou, K. Ahadi, Z. Nourbakhsh, and D. Vashaee, Topological quantum matter to topological phase conversion: Fundamentals, materials, physical systems for phase conversions, and device applications, [Materials Science and Engineering: R: Reports](#) **145**, 100620 (2021).
- [66] H. Nielsen and M. Ninomiya, A no-go theorem for regularizing chiral fermions, [Phys. Lett. B](#) **105**, 219 (1981).
- [67] S. L. Adler, Axial-vector vertex in spinor electrodynamics, [Phys. Rev.](#) **177**, 2426 (1969).
- [68] J. S. Bell and R. Jackiw, A PCAC puzzle: $\pi^0 \rightarrow \gamma\gamma$ in the σ model, [Nuovo Cim. A](#) **60**, 47 (1969).
- [69] H. Nielsen and M. Ninomiya, The Adler-Bell-Jackiw anomaly and Weyl fermions in a crystal, [Physics Letters B](#) **130**, 389 (1983).
- [70] P. Hosur and X. Qi, Recent developments in transport phenomena in Weyl semimetals, [Comptes Rendus Physique](#) **14**, 857 (2013).
- [71] D. T. Son and B. Z. Spivak, Chiral anomaly and classical negative magnetoresistance of Weyl metals, [Phys. Rev. B](#) **88**, 104412 (2013).
- [72] S. K. Yip, Kinetic equation and magneto-conductance for Weyl metal in the clean limit, [arXiv e-prints \(2015\)](#), [arXiv:1508.01010 \[cond-mat.str-el\]](#).
- [73] D. Xiao, J. Shi, and Q. Niu, Berry phase correction to electron density of states in solids, [Phys. Rev. Lett.](#) **95**, 137204 (2005).
- [74] C. Duval, Z. Horváth, P. A. Horvathy, L. Martina, and P. Stichel, Berry phase correction to electron density in solids and “exotic” dynamics, [Mod. Phys. Lett. B](#) **20**, 373 (2006).
- [75] D. T. Son and N. Yamamoto, Berry curvature, triangle anomalies, and the chiral magnetic effect in Fermi liquids, [Phys. Rev. Lett.](#) **109**, 181602 (2012).
- [76] M.-X. Deng, H.-J. Duan, W. Luo, W. Y. Deng, R.-Q. Wang, and L. Sheng, Quantum oscillation modulated angular dependence of the positive longitudinal magnetoconductivity and planar Hall effect in Weyl semimetals, [Phys. Rev. B](#) **99**, 165146 (2019).